

Cambridge University Press

978-1-107-41409-9 - Materials Research Society Symposium Proceedings: Volume 573:

Compound Semiconductor Surface Passivation and Novel Device Processing

Editors: H. Hasegawa, M. Hong, Z. H. Lu and S. J. Pearton

Excerpt

[More information](#)

---

**Part I**

**Fundamentals of Surfaces  
and Their Passivation**

Cambridge University Press

978-1-107-41409-9 - Materials Research Society Symposium Proceedings: Volume 573:  
Compound Semiconductor Surface Passivation and Novel Device Processing

Editors: H. Hasegawa, M. Hong, Z. H. Lu and S. J. Pearton

Excerpt

[More information](#)

---

Cambridge University Press

978-1-107-41409-9 - Materials Research Society Symposium Proceedings: Volume 573:

Compound Semiconductor Surface Passivation and Novel Device Processing

Editors: H. Hasegawa, M. Hong, Z. H. Lu and S. J. Pearton

Excerpt

[More information](#)

## THEORY OF THE SULPHUR-PASSIVATED InP(001) SURFACE

**LAURENT J. LEWIS**[a]

Département de physique et GCM, Université de Montréal, C.P. 6128, Succ. Centre-Ville, Montréal, Québec, Canada H3C 3J7

**CHANDRÉ DHARMA-WARDANA**[b]

Institute for Microstructural Sciences, National Research Council of Canada  
Ottawa, Ontario, Canada K1A 0R6

### ABSTRACT

We present a detailed and comprehensive theoretical investigation of the sulphur-passivated (001) surface of InP. First, the ground-state structure is determined using density-functional methods, including full relaxation of the surface. The lowest-energy structure at 0 K is a striking  $(2 \times 2)$  reconstruction with the S atoms displaced from the bridge sites to form short and long dimers, belonging to two distinct sublayers. This surface structure is used to calculate the backscattering Raman spectrum; the two peaks arising from surface-layer vibrations predicted by our calculations are observed. Next, our first-principles calculations are extended to the study of a number of other stable states of the surface that can arise upon annealing. For this purpose, we construct and relax several higher-energy states of the surface, and calculate the corresponding core-level photoemission spectra. A remarkable sequence of structures is found to unfold from the fully S-covered ground state as they become energetically accessible. The surface S atoms exchange with bulk P atoms, forming new (and strong) S-P bonds while dissociating pre-existing S-S dimers. The predicted core-level spectra are found to be entirely consistent with the experimental measurements; our calculations indicate that the annealed (at about 700 K) surface is a  $(2 \times 2)$  structure containing two S and two P atoms per unit cell. Finally, we have used the predicted stable surface structures to calculate the photoemission and inverse photoemission spectra. They are found to agree well with experiment if the surface is assumed to consist of a mixture of the above ground-state and annealed structures.

### INTRODUCTION

III-V compound semiconductors (GaAs, InP, etc.) are technologically important materials having many potential applications in devices such as solar cells, Schottky and laser diodes, and integrated optoelectronic circuits [1, 2]. These devices require chemically-stable surfaces or interfaces. This is assured in Si technology by surface oxidation; for III-V materials, however, the untreated surfaces are quite reactive due to the high density of surface states. Passivation methods employing sulphur overlayers have been developed to reduce the surface density of states of III-V compounds [3, 4], significantly improving the electronic properties of the surfaces.

An important step towards understanding passivation is the determination of the atomic structure of the surfaces. For InP(001)-S, it was suggested, on the basis of low-energy electron diffraction (LEED) and x-ray photoelectron spectroscopy (XPS) experiments [4], that the surface is terminated with a monolayer of sulphur, the S atoms occupying bridge sites and forming bonds to indium atoms only in a  $(1 \times 1)$  pattern. A further study using x-ray absorption near-edge structure (XANES) [5] suggested that the In-S-In bond angle was close to  $100^\circ$  — smaller than the ideal tetrahedral In-P-In bond angle ( $109.5^\circ$ ). In the analysis used in these initial experiments [4, 5], no surface relaxation was however considered.

We have determined the ground-state structure of the InP(001)-S surface [6] using first-principles total-energy minimization methods [7]. As discussed below, the surface is found to

Cambridge University Press

978-1-107-41409-9 - Materials Research Society Symposium Proceedings: Volume 573:

Compound Semiconductor Surface Passivation and Novel Device Processing

Editors: H. Hasegawa, M. Hong, Z. H. Lu and S. J. Pearton

Excerpt

[More information](#)

have two S sublayers separated by 0.22 Å; the top S sublayer contains monomer pairs sitting close to bridge sites, while the lower sublayer contains strongly-dimerized S pairs. Thus the S atoms exist in *two types of chemical environments*. This structure is quite different from the currently-accepted description of the more extensively studied GaAs-S surface [8], which our calculations confirm.

Core-level (CL) spectroscopy can distinguish an atom in different bonding situations since the core-level positions of atomic lines shift as a function of the chemical environment [9]. The method is a powerful tool for probing surface structure; this however requires theoretical predictions of the CL excitation energies (CL-E), in particular when different structures “compete” because, e.g., of annealing, surface preparation, etc., which may lead to structures other than the ground state. We have calculated the CL-E from first-principles in order to follow the evolution of the InP(001)-S surface upon annealing. The theory predicts a number of stable structures besides the ground which become energetically accessible upon annealing. In particular, surface S atoms exchange with bulk P atoms, forming new strong S-P bonds while dissociating pre-existing S-S dimers. Thus, we are lead to a picture wherein the InP(001)-S surface is actually a system which could contain a mixture of S, S and P, or P-terminated InP(001) domains, depending on the kinetics imposed by the annealing conditions. Our results are confirmed by calculations of the photoemission (PE) and inverse photoemission (IPE) spectra. We give full details of these surface configurations below, but first present the theoretical framework underlying the present calculations.

## COMPUTATIONAL FRAMEWORK

### Total-energy minimization

The total-energy minimization calculations were performed within the framework of density-functional theory (DFT) in the local-density approximation (LDA), using plane waves (PW) to expand the electron wavefunctions, together with non-local, norm-conserving pseudopotentials (PP) [10]. The electron exchange-correlation energy is taken to be of the Ceperley-Alder form [11]. Only the  $\Gamma$  point was used to sample the reciprocal space and a 10 Ry energy cutoff was employed in the plane-wave expansions. The validity of our pseudopotentials for In, P and S was verified on various molecular configurations [12, 13, 14].

The semi-infinite crystal with the InP(001) surface exposed to vacuum is modeled, for the total-energy minimization calculations, as a supercell slab containing six layers, each with four atoms. The first (topmost) layer contains four S (or P) atoms. The second contains four In atoms, as implied by the chemistry of the material and by recent experimental studies [4, 5]. Subsequent layers follow the zinc-blende structure, except the bottom one, which consists of four In atoms and two H atoms positioned in a  $(1 \times 2)$  pattern such as to saturate the dangling bonds [13]. The atoms in the bottom three layers are held fixed in their bulk positions, while the other atoms are allowed to relax so as to minimize the total energy. Periodic boundary conditions are applied in the  $x$ ,  $y$ , and  $z$  directions but a vacuum region of width 7.225 Å (equivalent to five bulk In-P interplanar distances) is used along  $z$ , i.e. normal to the surface. For the fixed layers we used the theoretical bulk lattice constant [13] of 5.78 Å which compares well with the experimental [15] value of 5.87 Å.

### Core-level excitation energies

Using the relaxed structures provided by the PW-PP calculations, the S-2*p* core-level spectra were determined using the all-electron full-potential-semi-relativistic (FP-SR) method [16]. In the core-level-excitation process, an electron in a core level (here S-2*p*) is knocked out by an incident photon and placed in an outgoing electron state. The “hole” left

Cambridge University Press

978-1-107-41409-9 - Materials Research Society Symposium Proceedings: Volume 573:

Compound Semiconductor Surface Passivation and Novel Device Processing

Editors: H. Hasegawa, M. Hong, Z. H. Lu and S. J. Pearton

Excerpt

[More information](#)

behind has an effective positive charge which interacts with the remaining atomic and band electrons, as well as with the outgoing electron. Thus, the photoionization process involves electronic relaxation effects in the initial state as well as in the final state. In photoionization experiments, the time scale of the relaxation is usually short and electronic relaxation has occurred by the time the kinetic energy of the outgoing electron is measured. Hence the measured core-level excitation energy involves initial-state as well as final-state relaxation effects; in our calculations, both are included.

We consider a photoemission experiment where the photon energy is  $h\nu$ , while the total energies of the initial and final states of the crystal are  $E_i$  and  $E_f$ . The measured kinetic energy  $E_{ke}$  of the photoelectron is such that  $h\nu = E_f - E_i + E_{ke}$  and the measured CL-E,  $\varepsilon_{2p} = E_f - E_i$ , is a property of the initial *and* final states of the system. Evaluation of the electronic excitation effects *via* many-body methods is a numerically very demanding task. It is important to note that the DFT (Kohn-Sham) eigenvalues are not excitation energies; nevertheless, the total-energy difference (TED) between the ground state and the “excited” state (i.e., with a core hole) can be taken as a measure of the CL-E. Another method that can provide a reasonable estimate of the CL-E is the “Slater transition-state” method (STS) [17]. It is numerically simple and is closely related to DFT. In STS, the  $2p$  core-hole energy includes both initial-state and final-state effects, and is shown (under certain assumptions) to be equal to the  $2p$  eigenvalue of the “transition state”, a state having a *half-occupied* core hole. We have used both TED and the STS method to calculate the CL energies. Full details of the calculations are given in Ref. [14]. The difference in the estimates from the two methods — about 0.5 eV — provides a theoretical “error bar”.

### Photoemission spectra

We have also calculated the photoemission (PE) and inverse photoemission (IPE) spectra of the energetically-probable surface structures obtained from our first-principles calculations, and compare them to the experimental data reported recently [18]. We have benchmarked our procedure using the (111) surface of silicon. As was the case for the CL spectra discussed above, the PE and IPE spectra were determined using the energy-minimized geometries obtained from first-principles. We thus constructed supercells containing typically 16 atomic layers which are then used to calculate the electronic band structure, here within the all-electron, full-potential-linear-muffin-tin-orbital (FP-LMTO) method [16].

The photoelectron current per unit solid angle in PE at photon energy  $\hbar\omega$  is given by

$$J^{\text{PE}}(E_{\text{kin}}, \omega) \propto \sqrt{E_{\text{kin}}} \sum_i W_{if}. \quad (1)$$

where  $E_{\text{kin}} = E_f - E_F - \phi$  ( $E_F$  is the Fermi energy and  $\phi$  is the workfunction) and  $W_{if}$  is the transition probability between initial and final states; it is given by the Fermi golden rule:

$$W_{if} = \frac{2\pi}{\hbar} |\langle f | H_{\text{int}} | i \rangle|^2 \delta(E_f - E_i - \hbar\omega). \quad (2)$$

Likewise, for the IPE current,

$$J^{\text{IPE}}(E_{\text{kin}}, \omega) \propto [1/\sqrt{E_{\text{kin}}}] \sum_f W_{fi} \quad (3)$$

where, now,  $E_{\text{kin}} = E_i - E_F - \phi$ . The transition matrix elements of Eqs. 1 and 3 are evaluated directly from the Kohn-Sham eigenstates appropriate to the occupied/unoccupied levels. Our calculations indicate that the DOS profile provides a poor approximation to the measured spectra; this is of some importance since experimental PE/IPE results are often

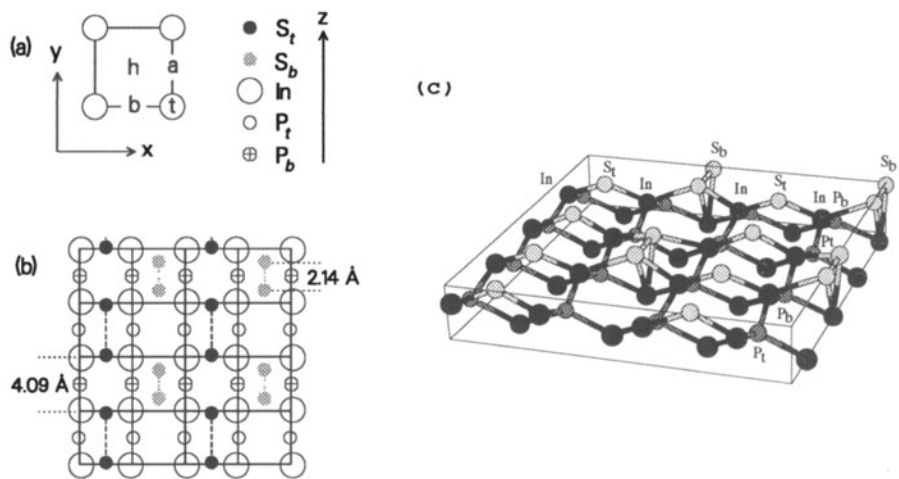


Figure 1: (a) Four possible sites for the S atom: bridge {b}; anti-bridge {a}; top {t} and hollow {h}. (b) Top view and (c) ball-and-stick model of the fully-relaxed S-passivated InP(001) surface.

presented as a mapping of the bandstructure of a material, which does not seem to be correct. Full details can be found in Ref. [19].

RESULTS

Ground-state structure

There are four possible arrangements for the S atoms which are consistent with the reported (1×1) pattern: “hollow”, “bridge”, “anti-bridge”, and “top” sites [cf. Fig. 1(a)]. Of these, the bridge-site structure is the most favourable if the (1×1) pattern is imposed, just as in the case of GaAs-S [8]. The ground-state structure provided by our first-principles simulations, however, is the (2×2) reconstruction depicted in Figs. 1(b) and (c). The surface S layer splits into two sublayers, each containing half the total sulphur. The top sublayer (S<sub>t</sub>) sublayer contains long dimers (“monomer pairs”), with the S atoms positioned close to bridge sites, but slightly displaced in the [1̄10] direction, yielding a S<sub>t</sub>-S<sub>t</sub> bond length of 3.82 Å. The bottom sublayer (S<sub>b</sub>), in contrast, contains strongly dimerized (along the [1̄10] direction) S pairs, with a bond length of 2.14 Å. The sequence of atomic planes (SAP) in the z-direction, with S<sub>t</sub> at the surface, may be presented as:

$$SAP = (In - P)_{bulk} - In - P_b - P_t - In - S_b - S_t \tag{4}$$

The interplaner distances near the surface region can be compared with the bulk In-P distance *d*<sub>0</sub> of 1.445 Å. The S<sub>t</sub> layer relaxes only 0.116 Å towards the bulk, while S<sub>b</sub> is displaced 0.22 Å below the S<sub>t</sub> layer. The In layer below S<sub>b</sub> remains integral while relaxing inwards; the following P layer, echoing the splitting of the top S layer, separates into two sublayers. The interplaner distances, starting from the left-most In-atom are: In-P<sub>b</sub> = 1.321 Å, while In-P<sub>t</sub> = 1.532 Å, giving an average In-(P<sub>b,t</sub>) distance of 1.427 Å. The other distances are

$P_t\text{-In} = 1.299 \text{ \AA}$ ,  $\text{In-S}_b = 1.169 \text{ \AA}$ , and  $\text{In-S}_t = 1.388 \text{ \AA}$ . We also recovered this ground state using a larger supercell with eight atoms per plane ( $x$ -dimension doubled). The surface thus loses its  $(1 \times 1)$  periodicity in favour of a  $(2 \times 2)$  pattern, with each short dimer surrounded by four long dimers, and *vice versa*. As we will see below, there are many metastable states on this surface.

The structure proposed on the basis of XANES [5] recovers the correct  $[\bar{1}10]$  orientation of the S-atoms, but not other details. According to our calculations, it does not in fact correspond to a local energy minimum, and lies some 0.5 eV above the ground state. However, a recent study [20] of the surface using scanning tunneling microscopy (STM) found that it has a locally ordered  $(2 \times 2)$  structure, as predicted by our model. In contrast, LEED measurements, which depend on long range order, show a  $(1 \times 1)$  pattern, in agreement with Tao et al. [4]. This is also consistent with our model: The In-layer just below the S-layer has a large electron-scattering cross section and retains a  $(1 \times 1)$  aspect in our structure.

In order to confirm the existence of the lowest energy structure predicted by our calculations, we have determined the Raman spectrum of the surface, which can then be compared to the experimental Raman spectrum (longitudinal vibrational modes along  $z$ ). In order to do this, we calculated the interplanar force constants in the “frozen-phonon” approach [21]. The lattice dynamics along [001] rigorously simplifies to a linear chain of masses, each node of the chain representing a rigidly-vibrating plane of atoms. The phonon modes were calculated using a slab of 1006 layers, with the top six layers having the sequence of atomic layers obtained above for the ground state. The calculated back-scattering Raman spectrum of the system [22] is shown in Fig. 2(a). The calculated *intensities* are, as usual, a qualitative measure of the relative strengths of the peaks; however, their *positions* are expected to be reliable to within a few wavenumbers. The “bulk” LO-phonon peak of InP is calculated to

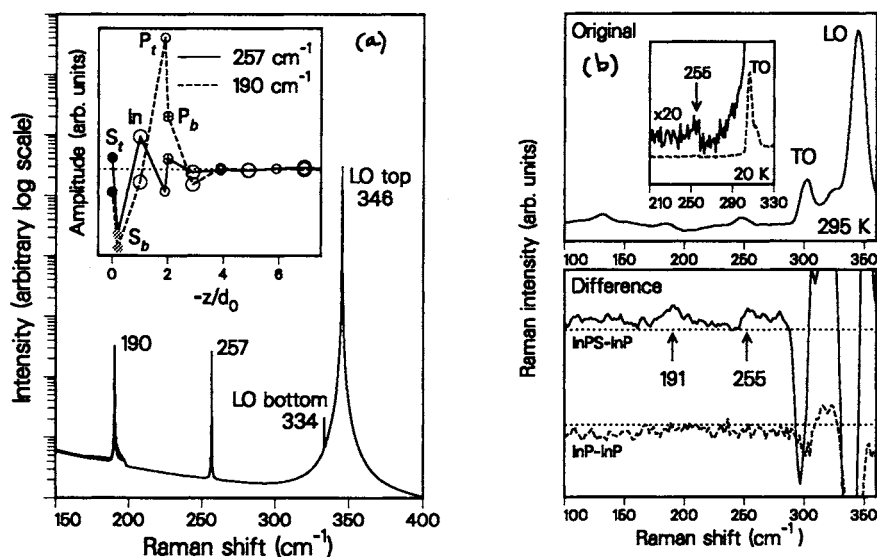


Figure 2: (a) Calculated Raman spectrum of the fully-relaxed InP(001)-S surface. The (longitudinal) vibrational amplitudes of the atomic planes are shown in the inset as a function of  $z/d_0$  ( $d_0 = 1.445 \text{ \AA}$ ). (b) Experimental Raman spectra of InP(001)-S at 295 and 20 K (inset).

Cambridge University Press

978-1-107-41409-9 - Materials Research Society Symposium Proceedings: Volume 573:

Compound Semiconductor Surface Passivation and Novel Device Processing

Editors: H. Hasegawa, M. Hong, Z. H. Lu and S. J. Pearton

Excerpt

[More information](#)

be at  $346 \pm 4 \text{ cm}^{-1}$  at 0 K, in excellent agreement with the experimental value at (20 K) of  $349 \pm 1 \text{ cm}^{-1}$ . The weak feature (note logarithmic intensity scale) at  $334 \text{ cm}^{-1}$  is the bottom of the LO-phonon branch and is not visible for periodic structures, but appears in our calculation since k-conservation fails in the presence of a surface.

Two modes which arise from the presence of the S-layer and the surface reconstruction were identified in the theoretical Raman spectrum, at  $190 \pm 2$  and  $257 \pm 3 \text{ cm}^{-1}$ . The phonon eigenvectors [displacements from equilibrium; cf. inset of Fig. 2(a)] indicate that for the mode at  $190 \text{ cm}^{-1}$ , the  $P_b$  and  $P_t$  sublayers displace in the *same* direction, with  $P_t$  having the largest amplitude, while the  $S_b$  and  $S_t$  sublayers also displace together but in the sense opposite to  $P_{b,t}$ . For the mode at  $257 \text{ cm}^{-1}$ , the  $S_b$  and  $S_t$ , as well as  $P_b$  and  $P_t$ , vibrate in *opposite* directions. Experimental observation of these two modes would evidently be strong evidence for the proposed structure, and in particular the distinctive splitting of the S and P layers produced by the  $(2 \times 2)$  reconstruction.

Since the contribution of the surface sulphur layer to the total spectrum is of order  $1/N$  ( $N$  = the number of layers traversed by the light probe), state-of-the-art light scattering techniques are called for. The Raman spectrum was measured in the quasi-backscattering configuration for a number of freshly prepared samples [20] at 295 K and 20 K. In order to isolate the very weak InP-S surface mode, the Raman spectrum of the bare InP(001) substrate recorded under identical conditions were subtracted from each InP(001)-S spectrum. Details of the experiment are given in Ref. [6].

The spectrum of an InP-S sample measured at 295 K is shown in the upper panel of Fig. 2(b); it is complicated by the presence of second-order Raman (SOR) lines below the transverse optic (TO) phonon. The inset shows the corresponding spectrum at 20 K, where the SOR are much reduced. The weak peak at  $255 \text{ cm}^{-1}$  is an order of magnitude weaker than the TO-phonon peak, which is itself weak in the back-scattering configuration. The lower panel of Fig. 2(b) shows “difference” spectra at 295K obtained by subtracting the untreated InP(001) spectrum from the InP(001)-S spectrum and averaging over 15 different runs for the same physical point on the surface. A peak-search routine, which applies a Poisson statistics analysis, detected peaks at  $191 \pm 1$  and  $255 \pm 1 \text{ cm}^{-1}$ , in remarkable accord with the theoretical (0 K) values of 190 and  $257 \text{ cm}^{-1}$ . The peaks are clearly seen in the top curve of the lower panel, whereas there is no such peak structure in the bottom curve, which is for the clean surface. Entirely equivalent results were obtained from other samples.

Our results are interesting in many respects; in particular, they show that the InP-S surface is quite different from that currently accepted for GaAs-S. Our structure, if used in calculations for GaAs-S, is in fact found to be a local minimum approximately 0.2 eV above the calculated ground state of GaAs-S. Clearly, results from GaAs-S studies cannot be simply carried over to the InP-S system, and *vice versa*.

### Core-level shifts

We examine here the effect of annealing on the structure of the surface, and give a systematic explanation of the observed CLS, complementing the Raman measurements presented above. Annealing opens an energy window whereby structures other than the ground state become statistically or kinetically accessible. In addition, this sets in motion diffusion processes where surface atoms migrate towards the bulk and *vice versa*.

The sequence of surface structures we considered is given in Fig. 3, where (a) is the ground-state geometry discussed above. We give, for each, the energy with respect to the lowest-energy structure at that coverage, but do not attempt to compare the lowest-energy structures at different coverages since that would require addressing the issue of how the sulphur atoms which migrate to the bulk arrange themselves. The corresponding theoretical S-2p excitation energies (from TED) are reported in Table I; the S atom with the core hole

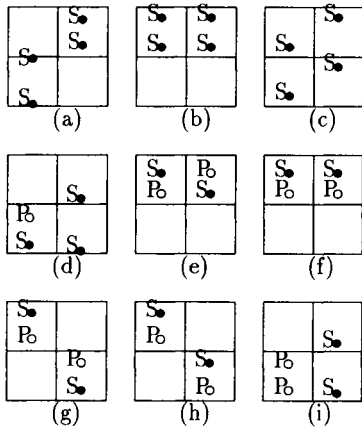


Figure 3: Top view of the fully-relaxed InP(001)-(S,P) surface structures. (a)-(c) are full S-covered; (d) is 3/4-S-covered; (e)-(i) are 1/2-S-covered.

Configuration	Structure	$\varepsilon_{2p}$ ( $\Delta E_g$ )
<i>Full S-coverage</i>		
(a) (ground-state)	$2 \times 2$	(0.0)
S*-S	monomer	161.9
S*-S	dimer	162.9
(b) (unstable)	$2 \times 1$	(0.86)
(c)	$2 \times 1$	(0.30)
S*-	monomer	161.6
<i>3/4-ml-S coverage</i>		
(d)	$2 \times 2$	(0.0)
S*-P	dimer	161.3
S*-S	monomer	160.6
<i>1/2-ml-S coverage</i>		
(e)	$2 \times 2$	(0.0)
S*-P	dimer	162.9
(f)	$2 \times 1$	(0.17)
S*-P	dimer	163.6
(g)	$2 \times 2$	(0.135)
S*-P	dimer	163.0
(h)	$2 \times 2$	(0.046)
S*-P	dimer	162.8
(i)	$2 \times 2$	(1.0)
S*-S	monomer	161.6

Table I: CL energies  $\varepsilon_{2p}$  (eV) for the surfaces of Fig. 3, and ground-state energies  $\Delta E_g$  [per  $(2 \times 2)$  cell, in eV] relative to the lowest-energy structure at each coverage. S\* is the atom with the 2p core-hole.

is marked S\*. Two different spectra are expected in structures with two inequivalent S atoms. Further, each S-2p level is a relativistic doublet and hence each spectrum is expected to show a double-peak structure. The spin-orbit splitting was calculated using the method of Koelling *et al.* [23] in the all-electron FP-SR LDA scheme (see Ref. [14] for details). It was found to be equal to 1.29 eV ( $\Delta\varepsilon = -0.86$  eV for  $j=1/2$  and  $+0.43$  eV for  $j=3/2$ ). The two peaks of the doublet have intensities 1:2 since the level degeneracies are  $2j + 1 = 2$  and 4. The lineshapes were assumed to have a Lorentz-Gauss (Voigt) profile; no attempt was made to provide a first-principles spectral lineshape. The relative intensities of the two peaks in the doublet, however, was forced by the degeneracies  $2j + 1$  discussed above.

A  $(2 \times 1)$  reconstruction has been reported on the basis of photoemission and LEED studies of annealed samples by Mitchell *et al.* [18] and was assigned to the structure of Fig. 3(b), containing S dimer rows. Our calculations show that this geometry is unstable, i.e., not even an energy minimum. However, local energy minima do exist, e.g., Fig. 3(c), which has just one type of S atoms [6], lying  $\sim 0.07$  eV per S atom above the ground state. LEED and STM may have difficulty in distinguishing P and S atoms on surfaces with partial (S,P) coverages as in, say, Fig. 3(d)-(i), while CL spectroscopy has no such difficulty since S-2p and P-2p excitations are well separated. A stringent test of the  $(2 \times 2)$  structure is, therefore, to compare the *predicted* dimer and monomer CL spectra against experiment. This would distinguish the surface from the  $(1 \times 1)$  structure analogous to the GaAs(001)-S [8], where the S atoms are at bridge sites, and from the  $(2 \times 1)$  structure of Fig. 3(c), since they have only one type of sulphur.

Cambridge University Press

978-1-107-41409-9 - Materials Research Society Symposium Proceedings: Volume 573:

Compound Semiconductor Surface Passivation and Novel Device Processing

Editors: H. Hasegawa, M. Hong, Z. H. Lu and S. J. Pearton

Excerpt

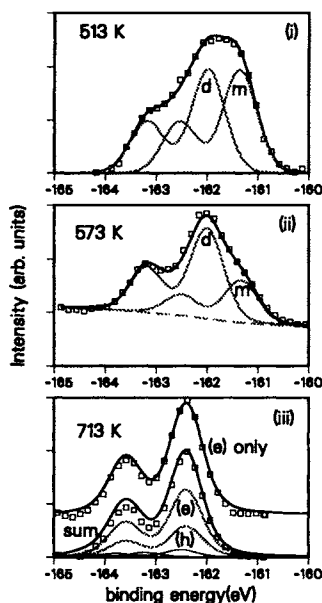
[More information](#)

Figure 4: Calculated (lines) and measured (squares) CL spectra of InP(001)-(S,P) at three different temperatures. The electron background is shown in (ii).

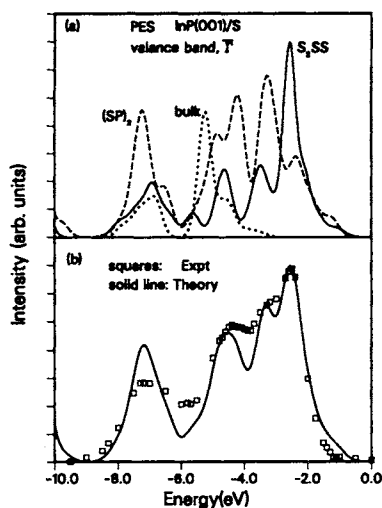


Figure 5: Calculated (lines) and measured (squares) PE spectra of InP(001)-(S,P): (a) individual and (b) composite PE spectra, as discussed in the text.

Photoelectron-spectroscopy measurements (carried out at the Stanford Synchrotron Radiation Laboratory) were taken at three different temperatures — 513, 573 and 713 K — and are displayed in Fig. 4. Details of the experiment can be found in Ref. [14]. Since Fig. 3(a) is the most likely structure, we analyse the low-T spectrum as follows. We assume that long-dimer sulphur atoms (“monomer” – ‘m’) and short-dimer atoms (“dimer” – ‘d’) contribute equally to the spectrum. Hence we have two equal-intensity doublets with the same s-o splitting, lineshape and a 1:2 intensity ratio in each doublet, as discussed above. With these strong constraints, the experimental profile is fitted with the two doublets (four Voigt profiles) whose peak positions are adjusted from the theoretical values only to within the expected error of  $\pm 0.5$  eV. The resulting fitted peak positions are designated the *experimental* peak values. The experimental s-o splitting is 1.18 eV; this will be used in displaying other data. On fitting the experimental data at 513 K, the *2p* experimental binding energies of ‘d’ and ‘m’ S atoms were found to be  $-162.57$  and  $-161.95$  eV, comparing very well with the theoretical values of  $-162.9$  and  $-161.9 \pm 0.5$  eV for the structure of Fig. 3(a). The experimental spectrum at 513 K is thus *clearly consistent* with the predicted  $(2 \times 2)$  ground-state structure.

On heating, other configurations begin to compete with the ground state. The next stable, fully-S-covered structure is that of Fig. 3(c). This structure gives a single S-*2p* CL-E calculated to be  $\sim -161.6$  eV, i.e., near the previous ‘m’ peak. If this is formed on heating, the ‘d’ intensity should decrease while the ‘m’ peak grows. Fig. 4(ii) shows that the monomer peak has, rather, decreased in intensity. Thus the structure of Fig. 3(c) does not form, because of other competing processes. Such a process is the surface-S $\leftrightarrow$ bulk-P exchange;